

2018-01-01

# Carbon nanotube-reinforced smart composites for sensing freezing temperature and deicing by self-heating

Jang, Sung-Hwan

<http://hdl.handle.net/10026.1/12322>

---

10.1177/1847980418776473

Nanomaterials and Nanotechnology

SAGE Publications (UK and US)

---

*All content in PEARL is protected by copyright law. Author manuscripts are made available in accordance with publisher policies. Please cite only the published version using the details provided on the item record or document. In the absence of an open licence (e.g. Creative Commons), permissions for further reuse of content should be sought from the publisher or author.*

# Carbon nanotube-reinforced smart composites for sensing freezing temperature and deicing by self-heating

Sung-Hwan Jang<sup>1</sup> and Yong-Lae Park<sup>2,3,4</sup>

## Abstract

Carbon nanotube-reinforced polymer composites were fabricated by high shear mixing. The microstructure and the electrical properties of the carbon nanotube–polymer composites were investigated by scanning electron microscopy and electrical resistance measurement. We found that the carbon nanotube composites showed high electrical conductivity ( $1.5 \text{ S m}^{-1}$ ) at 7.0 wt% of carbon nanotubes, and the increase in thickness enhanced the electrical conductivity of the composites. The multifunctional properties of the carbon nanotube composites were also investigated for use in sensing the freezing temperature and also in deicing by self-heating. The results showed that the carbon nanotube–polymer composites had high temperature sensitivity in the freezing temperature range from  $-5$  to  $5 \text{ C}$  and an excellent heating performance due to the Joule heating effect. The carbon nanotube composites are promising to be used as smart coating materials for deicing by self-heating as well as by detection of the freezing temperature.

## Keywords

Carbon nanotube, polymer composite, electrical conductivity, temperature sensing, Joule heating

Date received: 14 July 2017; accepted: 30 December 2017

Topic: Special Collection: High Performance and Smart Nano Engineered Composites for Civil Infrastructures

Topic Editor: Elisabetta Comini

Associate Editor: Filippo Ubertini

## Introduction

Smart composites have gained attention to a wide range of industrial applications in the areas of civil, mechanical, and aerospace engineering due to their potential in sensor-integrated systems with simultaneous environmental sensing, such as sensing of changes in strain, pressure, and temperature. They also make it easy to construct a light-weight structure integrated with various functionalities without additional equipment.

Carbon-based materials, such as carbon nanotubes (CNTs), carbon black, and graphene, have been widely used as fillers in different types of matrices in order to achieve smart composites.<sup>1–4</sup> In particular, CNTs are one of the promising materials that can provide excellent electrical, thermal, and mechanical properties. Because CNTs have much higher aspect ratios compared to other

carbon-based materials, a relatively small amount of CNTs can make the composite electrically conductive.<sup>5–7</sup> Therefore, CNT-reinforced composites have been widely used for different applications, such as structural components

<sup>1</sup> Department of Civil and Coastal Engineering, School of Engineering, University of Plymouth, Drake Circus, Plymouth, UK

<sup>2</sup> Department of Mechanical and Aerospace Engineering, Seoul National University, Gwanak-gu, Seoul, South Korea

<sup>3</sup> Institute of Advanced Machines and Design, Seoul National University, Gwanak-gu, Seoul, South Korea

<sup>4</sup> Robotics Institute, Carnegie Mellon University, Pittsburgh, PA, USA

## Corresponding author:

Yong-Lae Park, Department of Mechanical and Aerospace Engineering, Seoul National University, 1 Gwanak-ro, Gwanak-gu, Seoul 08826, South Korea.

Email: ylpark@snu.ac.kr



and sensing and heating elements.<sup>8–11</sup> For example, Shindo et al.<sup>12</sup> have examined the electromechanical response of a cracked CNT/polymer composite under tensile loading for crack detection based on the relationship between the electrical resistance and the crack length. Lee and Jeong<sup>13</sup> synthesized a sulfonated poly(1,3,4-oxadiazole)/multiwalled CNT composite film for a thermally stable high-performance composite and showed high electric heating efficiency.

In addition to strain sensing, composites reinforced with carbon-based materials can be used as temperature sensors and self-heating elements.<sup>14–18</sup> These composites belong to a type of electrical resistor that is sensitive to temperature and can transform electrical energy to thermal energy. For instance, Blasdel et al.<sup>19</sup> have characterized a fabric, which consisted of multiwalled CNTs and polypyrrole, for temperature sensing. They found that the nanocomposite materials acted like a temperature detector based on the resistance change that was linearly proportional to temperature change. Galao et al.<sup>20</sup> have investigated carbon fiber-reinforced concrete for deicing applications when used as a heating element although it required relatively long heating time. However, the abovementioned results were limited to a single function that is either temperature sensing or heating.

In this study, we introduce CNT-reinforced composite as a smart coating system that can be applied to civil infrastructures for simultaneous sensing and actuation by detecting the freezing temperature and by self-heating, respectively. CNT-reinforced polymer composites with different CNT concentrations and film thicknesses were fabricated by high shear mixing. Then, influences of the film thickness and the CNT concentration on both the electrical conductivity and the temperature sensitivity were investigated. The self-heating capability of the composites by Joule heating was also examined. The results showed that CNT-reinforced polymer composites have the ability to serve as a promising smart coating material in civil infrastructures for sensing the freezing temperature and deicing by self-heating simultaneously in a cold weather.

## Experiments

### Materials

Multiwalled CNTs produced by thermal chemical vapor deposition were obtained from Nanolab (Waltham, Massachusetts, USA), which showed an average length and a diameter of 15.0  $\mu\text{m}$  and 10.0 nm, respectively. For matrix, polydimethylsiloxane (PDMS, Sylgard 184 Silicone Elastomer) consisting of a base elastomer (part A) and a curing agent (part B) was purchased from Dow Corning (Midland, Michigan, USA). All the materials were used as received.

### Fabrication of CNT/PDMS composite films

CNT/PDMS composite films were fabricated by high shear mixing. Different concentrations (approximately 0–10.0 wt%) of CNTs were carefully weighed with a precision weight scale and directly mixed with part A of the PDMS using a centrifugal mixer (ARE 301, Thinky Corporation, Tokyo, Japan) at a rotation speed of 2200  $\text{r min}^{-1}$  for 3 min. Part B of the PDMS was added into the mixture with a weight ratio of 10:1 and then mixed again using the same mixer for another 3 min. Then, the mixture was painted layer by layer onto a glass substrate with a brush, followed by degassing under vacuum for 20 min in order to eliminate the air bubbles captured in the matrix that generally could cause low electrical conductivity than desired. This layer-by-layer process facilitates fabrication of multilayered CNT composite films, yielding high electrical conductivity and high mechanical strength due to the increased density of the CNT microstructure. This process was repeated until the desired thickness or the desired number of layers was achieved. Finally, the mixture was cured at 100°C for 1 h in a convection oven. Then, the cured CNT/PDMS composite films were left at room temperature for further cooling and curing for a day.

### Characterizations

The thickness of the CNT/PDMS composite film was measured by a digital caliper. The microstructure of the composite film was observed using a scanning electron microscopy (FEI Sirion 600, JEOL, Tokyo, Japan).

The electrical resistance of the composite was measured by a two-point probe method using two different digital multimeters at room temperature. The high resistance above  $10^9 \Omega$  of the composites was measured by a high resistance meter (Keithley 6517B, Solon, Ohio, USA), whereas nominal resistance of the composites was measured by a precision multimeter (Fluke 8845A Everett, Washington, USA). Then, the electrical conductivity of the composite was calculated as  $\sigma = L/AR$ , where  $A$  and  $L$  are the area and the length of the sample, respectively, and  $R$  is the resistance. The temperature dependence of the electrical properties was measured by placing the samples in a lab freezer. A set of five specimens was used for each test to evaluate the electrical properties.

For heating performance by Joule heating, a direct current power supply (Sorensen XPH35-4D, San Diego, California, USA) was used to provide heat by controlling the input voltage. Figure 1(a) shows the experimental setup. Two pieces of copper tape ( $25 \times 25 \text{ mm}^2$ ) were attached to both ends of the CNT composite film to be used as electrodes, and the input voltage (approximately 0–50 V) was applied to the composite to induce heat, creating uniform heat distribution, as shown in Figure 1(b). A temperature profile was obtained using a digital thermocouple logger (SL500TC, Supco, Manasquan, New Jersey, USA). In addition, thermal images of the samples

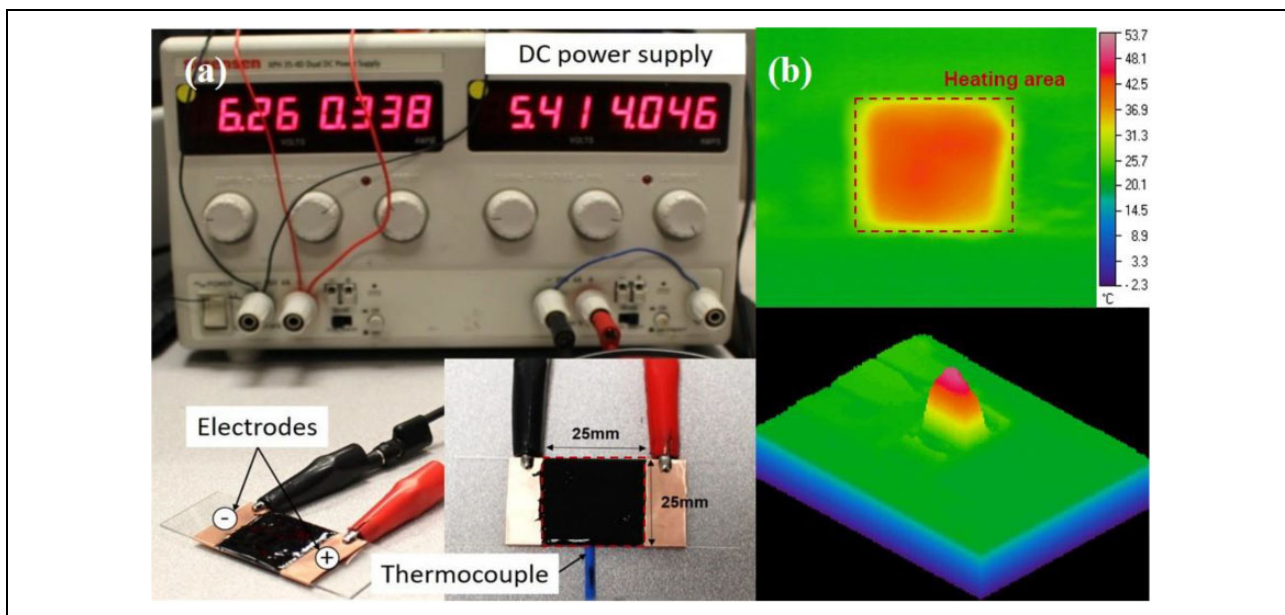


**Figure 1.** (a) Experimental setup for Joule heating and (b) uniform heat distribution of CNT/PDMS composite film. CNT: carbon nanotube; PDMS: polydimethylsiloxane.

during Joule heating were recorded using a thermal infrared camera (FLIR A325sc LWIR Wilsonville, Oregon, USA) for heat distribution.

For the defrosting performance, Joule heating was applied to the CNT/PDMS composite films (7.0 wt% CNT with 0.75 mm thickness) coated on a glass slide in the area of  $50 \times 50 \text{ mm}^2$ . Then, the sample was immersed into a water bath and frozen at  $-15^\circ\text{C}$  in a refrigerator for 24 h to clearly form the frost on the surface. The initial resistance of the CNT/PDMS film was approximately  $500 \ \Omega$ , and a voltage of 30 V was applied to the film to internally increase the temperature by Joule heating.

## Results and discussion

### Electrical conductivity

Figure 2 shows the electrical conductivities of the CNT/PDMS composite films as a function of CNT concentration. At low concentration, lower than 5.0 wt% of CNTs, the composites showed no conductivity due to lack of conductive networks of CNTs. The electrical conductivity of the composites rapidly increased by six orders of magnitude when the CNT concentration reached 5.0 wt% based on the increase in the CNT networks, as shown in Figure 3. The percolation threshold is a region where the composites transform from an insulator to a conductor through the connected CNT networks, which has been observed in the previous research.<sup>21–23</sup> After the percolation threshold, the electrical conductivity of the CNT/PDMS composite films gradually increased approaching  $1.5 \text{ S m}^{-1}$  as the CNT concentration increased. Based on our result, the CNT/PDMS films showed high electrical conductivity at

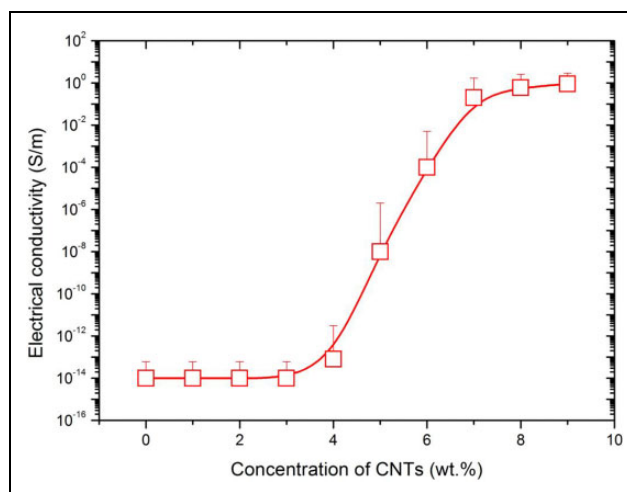


**Figure 2.** Electrical conductivity of CNT/PDMS composite films with varied CNT concentrations. CNT: carbon nanotube; PDMS: polydimethylsiloxane.

7.0 wt% of CNTs. Therefore, the CNT concentration was maintained at 7.0 wt% for further experiments.

### Influence of films' thickness on electrical conductivity

To check the influence of the film thickness on the electrical property (i.e. resistance or conductivity) of CNT-reinforced polymer composites, we prepared composite films with different thicknesses of 7.0 wt% of CNTs using the layer-by-layer fabrication. Figure 4 shows the resistance and conductivity change of the CNT/PDMS composite films as a function of thickness. As expected, the resistance of the films significantly decreased as the

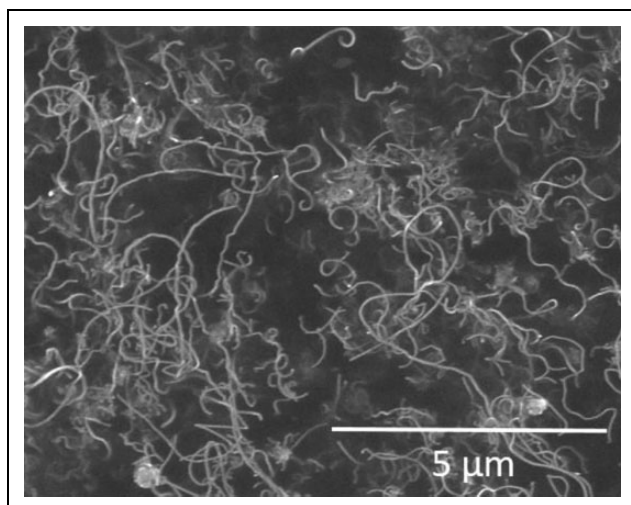


**Figure 3.** Microstructure of CNTs in the matrix. CNT: carbon nanotube.

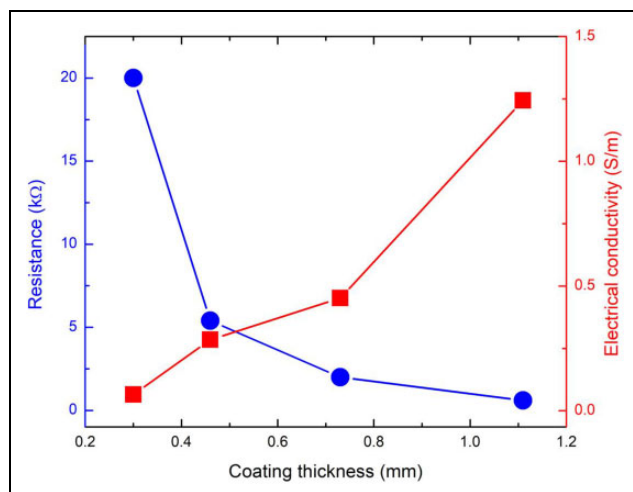


**Figure 4.** Resistance change and electrical conductivity of CNT/PDMS composite films with varied thicknesses. CNT: carbon nanotube; PDMS: polydimethylsiloxane.

thickness of the CNT/PDMS composite films increased. The electrical conductivity of the film was calculated by  $\sigma = L/AR$  based on the given resistance and different thicknesses of the films. It was found that the electrical conductivity showed a monotonic increase as the thickness increased. The highest electrical conductivity was  $1.25 \text{ S m}^{-1}$  for the 1.1-mm-thick CNT film, which was about 20 times higher than that of the 0.3-mm-thick CNT film. The electrical conductivity of the CNT film is mostly determined by the density of the conducting channels in a random CNT network, which is expected to be proportional to the concentration of low-resistance inter-tube junctions formed by CNTs.<sup>24,25</sup> By controlling the thickness by the layer-by-layer fabrication, it was expected that higher density of the CNT networks could be achieved with an increase of thickness, consequently, leading to an increase of the electrical conductivity of CNT/PDMS films.

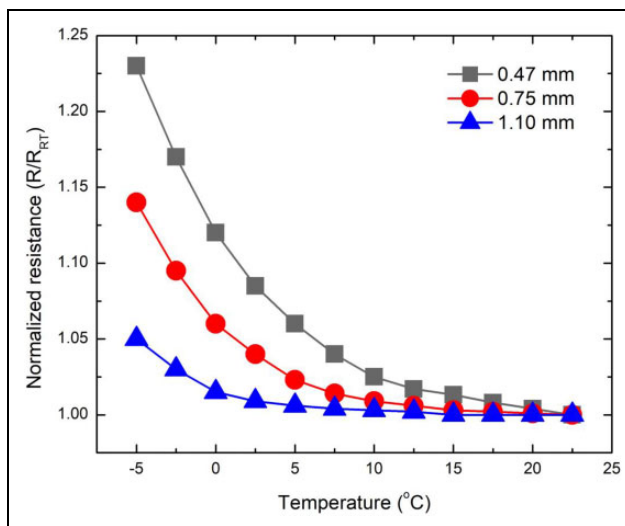


**Figure 5.** Change in resistance of CNT/PDMS composite films as a function of the temperature for different thicknesses. CNT: carbon nanotube; PDMS: polydimethylsiloxane.

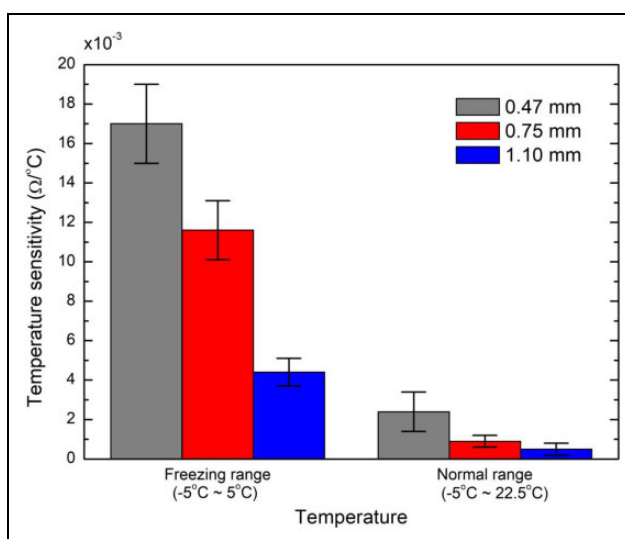


**Figure 6.** Temperature sensitivity of CNT/PDMS composite films with varied thickness. CNT: carbon nanotube; PDMS: polydimethylsiloxane.

### Detection of freezing temperature

The resistance change of the CNT/PDMS composite films was investigated. Figure 5 shows that temperature decreased from room temperature to  $-5^\circ\text{C}$  for simulating the weather during winter. All CNT/PDMS films with different thicknesses showed nonlinear electrical responses with the given temperature changes and decrease in resistance with temperature drops at certain rates, which is called a negative temperature coefficient (NTC). NTC is often reported in CNT-reinforced polymer composites, which depends on several factors, such as the characteristics of the polymer and the aspect ratio of CNTs.<sup>26–28</sup>

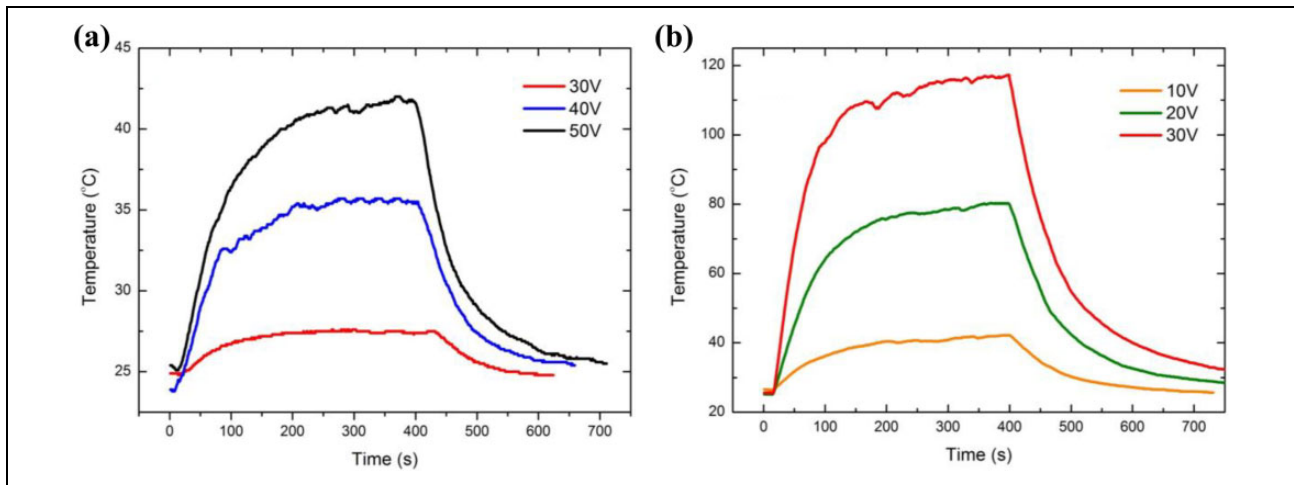


**Figure 7.** Temperature profiles of CNT/PDMS composite films with varied input voltages: (a) 0.47-mm CNT film and (b) 1.10-mm CNT film. CNT: carbon nanotube; PDMS: polydimethylsiloxane.

Therefore, NTC of the CNT/PDMS films can be used as a metric of smart coating materials for detecting the freezing temperature during winter.

Figure 6 shows the temperature sensitivity of the CNT/PDMS films with different thicknesses at different temperature ranges. The temperature sensitivity of the CNT/PDMS film was calculated by  $\Delta = (R - R_{RT})/T$ , where  $R$  is the resistance at a given temperature,  $R_{RT}$  is the resistance at room temperature, and  $T$  is the temperature. The CNT/PDMS composite films showed much higher temperature sensitivity in a small temperature range from  $-5^{\circ}\text{C}$  to  $5^{\circ}\text{C}$  rather than in the normal temperature range from  $5^{\circ}\text{C}$  to  $22.5^{\circ}\text{C}$ . Also, the influence of the thickness on the temperature sensitivity was investigated using three different film thicknesses. The sample with a low thickness (0.47 mm) showed the highest temperature sensitivity ( $0.017 \Omega^{\circ}\text{C}^{-1}$ ) in the range of the freezing temperature, which is almost 1.5 times and 18.9 times higher than that of the samples with the coating thickness of 0.75 and 1.10 mm, respectively. Therefore, by controlling the thickness of the film, CNT/PDMS composite films can be used for detecting the freezing temperature during winter based on high temperature sensitivity in a small temperature range.

### Self-heating performance

To demonstrate the potential as a heating element, the self-heating performance of the CNT/PDMS composite films was characterized in terms of the temperature profile in relation to the applied voltage. The power increased according to  $P = IV = V^2/R$ , where  $V$  is the applied voltage,  $I$  is the applied current, and  $R$  is the resistance of the CNT film, which is converted to heat through Joule heating effect.<sup>29–31</sup> In this study, we prepared CNT/PDMS composite films onto a glass slide with an area of  $25 \times 25 \text{ mm}^2$

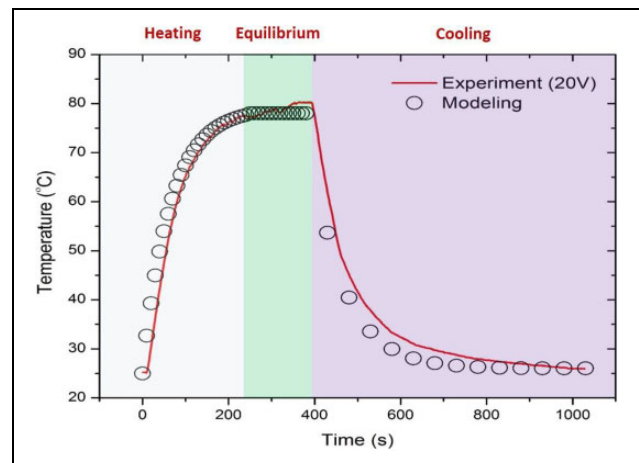


**Figure 8.** Analytical modeling for heating performance of CNT/PDMS composite films. CNT: carbon nanotube; PDMS: polydimethylsiloxane.

**Table 1.** Characteristics of heat model for CNT films with different thicknesses.

Thickness of CNT films (mm)	Characteristics of heating model		
	$t_g$	$q$	$t_d$
0.47	75	60	16.4
0.75	73	70	10.1
1.10	70	78	5.5

CNT: carbon nanotube.

with different coating thicknesses by the layer-by-layer fabrication. Then, different voltages were applied to the specimens for 15 min.

Figure 7(a) shows the temperature profiles of the 0.47-mm-thick CNT/PDMS composite films. It was clearly seen that the temperature of all the CNT/PDMS composite

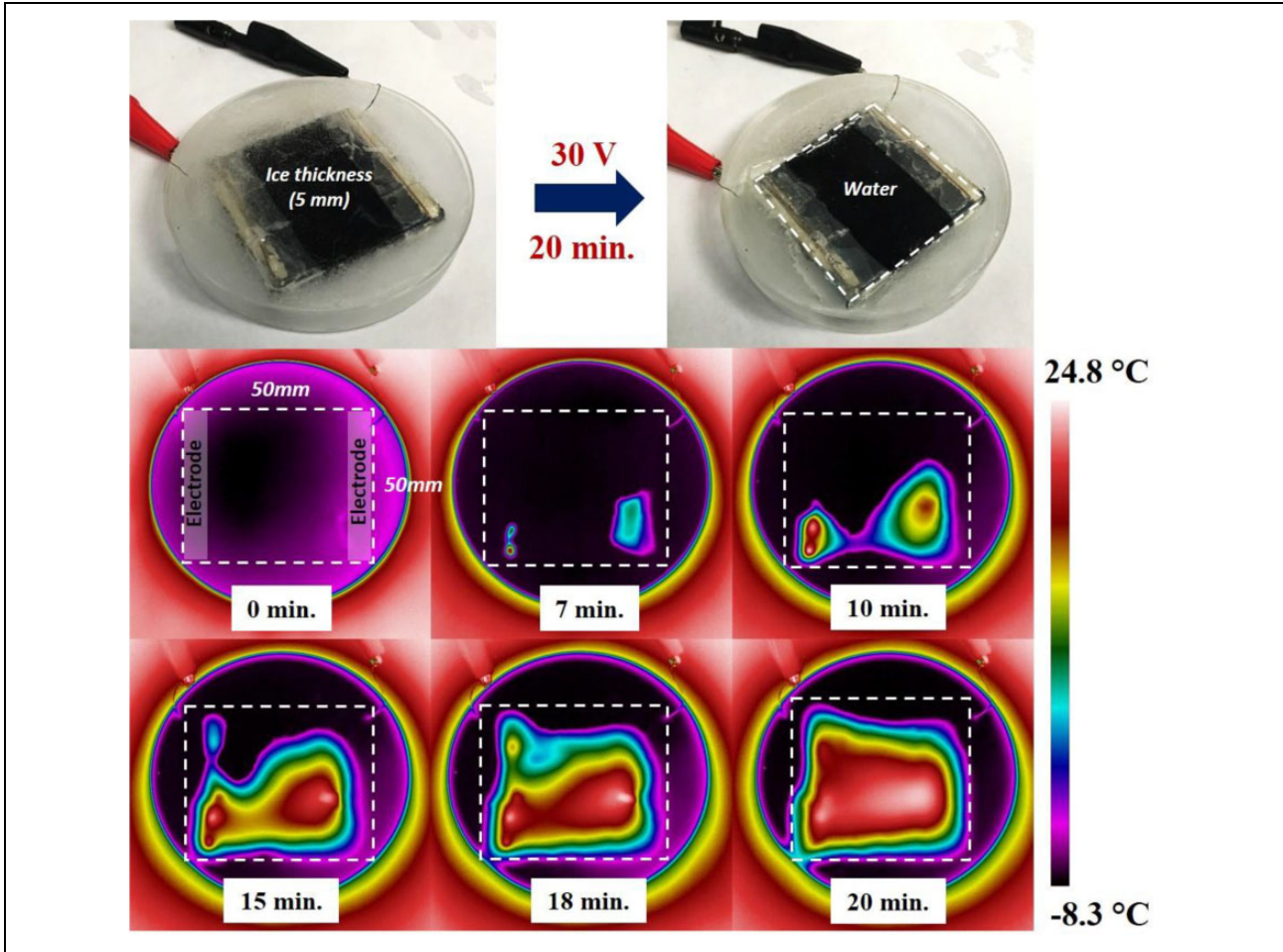


**Figure 9.** Defrost performance of CNT/PDMS composite film coated on glass. CNT: carbon nanotube; PDMS: polydimethylsiloxane.

films increased with increased voltages due to Joule heating. Maximum temperatures of 27 and 35°C were obtained at voltages of 30 and 40 V, respectively. Also, moderate temperature increases such as 42°C were observed at a higher voltage of 50 V. However, dramatic temperature increase was observed in the 1.10-mm-thick CNT/PDMS composite films, as shown in Figure 7(b). For instance, the maximum temperature of over 110°C was obtained at 30 V, which is much higher than that of 0.45-mm-thick CNT/PDMS film at the same voltage. This is attributed to the high electrical conductivity of the thick CNT/PDMS film supported by Figure 4. Moreover, the CNT films were able to reach high temperature, such as 100°C, without any change in resistance. Therefore, the CNT/PDMS film with high thickness may be useful for providing more heat at a relatively low voltage. In our experiments, the temperature went up rapidly compared to other conventional heating methods.<sup>32</sup>

The temperature evolution of the CNT/PDMS composite films by Joule heating can be theoretically modeled, which could be divided into different stages, such as

heating, equilibrium, and cooling, that can be shown with the following equations<sup>33</sup>

$$\frac{T_t - T_i}{T_{\max} - T_i} = 1 - e\left(\frac{-t}{t_g}\right) \quad (\text{heating stage}) \quad (1)$$

$$q = \frac{P_{\text{in}}}{T_{\max} - T_i} \quad (\text{equilibrium stage}) \quad (2)$$

$$\frac{T_t - T_i}{T_{\max} - T_i} = e\left(\frac{-t}{t_d}\right) \quad (\text{cooling stage}) \quad (3)$$

where  $T_i$  is the initial temperature,  $T_{\max}$  is the steady-state maximum temperature,  $T_t$  is the arbitrary temperature at time  $t_g$  which is the characteristic growth time constant,  $q$  is the equilibrium heat,  $P_{\text{in}}$  is the applied power,  $t_f$  is the final temperature, and  $t_d$  is the characteristic decay time constant. Figure 8 shows the comparison between the analytical solution and the experimental results from the 1.1-mm-thick CNT film at 20 V. Table 1 presents the change in the characteristics for the analytical model at each stage. Both  $t_g$  and  $q$

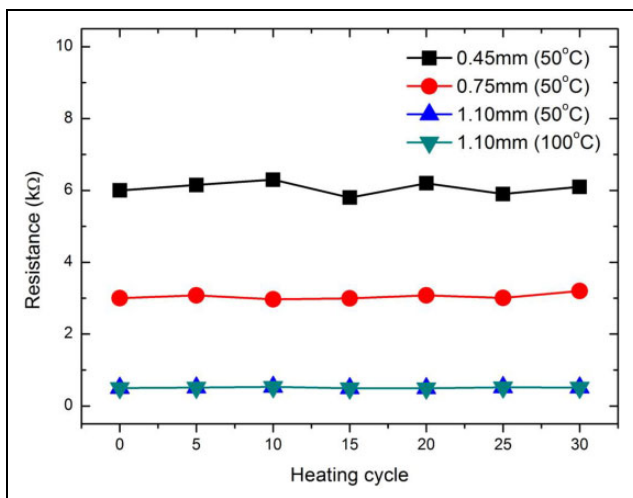


**Figure 10.** Change in resistance of CNT/PDMS composite films at heating cycle. CNT: carbon nanotube; PDMS: polydimethylsiloxane.

decreased, but  $t_d$  increased as the thickness of CNT/PDMS composite film increases.

Figure 9 shows the defrost performance of the CNT/PDMS composite films. The thickness of the ice on the CNT film was about 5 mm, and the temperature was  $-8.5^\circ\text{C}$ . Then, the 30.0 V was applied to both electrodes of the CNT/PDMS composite film. At 7 min of heating, the amount of heat was initially observed at the interface of the CNT/PDMS film and the electrode due to the higher electrical conductivity of the electrode. Also, it is noted that the nonuniform heat distribution during Joule heating attributed to different frost thicknesses. At 20 min of the heating, it was clear that the frost on the CNT/PDMS film was completely melted to water. Finally, Figure 10 shows the resistance change of the CNT/PDMS composite films by cyclic heating up to 30 cycles. All the CNT/PDMS films showed stable resistance retention at 30 heating cycles. Also, it was clearly seen that the CNT film showed stable heat resistance at an even higher heating temperature (approximately  $100^\circ\text{C}$ ).

## Conclusions

This study showed the feasibility of CNT-reinforced polymer composites for smart coating systems capable of detecting the freezing temperature and self-heating. Electrically conductive CNT/PDMS composite films were fabricated using a centrifugal mixing method. The results confirmed that the electrical conductivity of the CNT/PDMS composite films increased as both the CNT concentrations and the thickness of the film increased. It was also shown that the nonlinear change in resistance of all CNT/PDMS composite film samples was observed with decrease of temperature. Moreover, the CNT/PDMS composite films with a lower thickness showed a higher temperature sensitivity in the freezing temperature range from  $-5$  to

$5^\circ\text{C}$ . The self-heating performance of the CNT/PDMS composite films was investigated by the Joule heating effect. The thickness of the CNT/PDMS films significantly affected the temperature profile when a constant voltage was applied. The Joule heating effect was modeled using an analytic solution to predict the temperature profile of the CNT/PDMS composite films. Finally, we demonstrated the defrost performance of the CNT/PDMS composite film coated onto a glass slide which was covered with 5.0-mm-thick ice. The CNT/PDMS composite films successfully melted the ice on the glass in a short period of time. Therefore, we believe that CNT/PDMS composite films have a potential in various types of smart coating systems for detecting the freezing temperature and deicing by self-heating in civil infrastructures.

## Acknowledgments

This authors thank Samsung Global Research Outreach Program (Award number: A017519), Transport Technology Research Innovation Grant (T-TRIG), and Okawa Foundation Research Grant Award for the support.

## Declaration of conflicting interests

The author(s) declared no potential conflicts of interest with respect to the research, authorship, and/or publication of this article.

## Funding

The author(s) disclosed receipt of the following financial support for the research, authorship, and/or publication of this article: This work was supported in part by the Samsung Global Research Outreach Program (award no. A017519), in part by the Transport Technology Research Innovation Grant (T-TRIG), and in part by the Okawa Foundation Research Grant Award.

## References

- Frank S, Poncharal P, Wang ZL, et al. Carbon nanotube quantum resistors (in English). *Science* 1998; 280(5370): 1744–1746.
- Baughman RH, Zakhidov AA and de Heer WA. Carbon nanotubes—the route toward applications (in English). *Science* 2002; 297(5582): 787–792.
- Veedu VP, Cao A, Li X, et al. Multifunctional composites using reinforced laminae with carbon-nanotube forests (in English). *Nature Mater* 2006; 5(6): 457–462.
- Matos CF, Galembeck F and Zarbin AJG. Multifunctional materials based on iron/iron oxide-filled carbon nanotubes/natural rubber composites (in English). *Carbon* 2012; 50(12): 4685–4695.
- Li J, Ma PC, Chow WS, et al. Correlations between percolation threshold, dispersion state, and aspect ratio of carbon nanotubes (in English). *Adv Funct Mater* 2007; 17(16): 3207–3215.
- Wen M, Sun X, Su L, et al. The electrical conductivity of carbon nanotube/carbon black/polypropylene composites prepared through multistage stretching extrusion (in English). *Polymer* 2012; 53(7): 1602–1610.

7. Ayatollahi MR, Shadlou S, Shokrieh MM, et al. Effect of multi-walled carbon nanotube aspect ratio on mechanical and electrical properties of epoxy-based nanocomposites (in English). *Polym Test* 2011; 30(5): 548–556.
8. Wichmann MHG, Buschhorn ST, Gehrman J, et al. Piezoresistive response of epoxy composites with carbon nanoparticles under tensile load (in English). *Phys Rev B* 2009; 80(24): 245437-1-8.
9. Downey A, D'Alessandro A, Baquera M, et al. Damage detection, localization and quantification in conductive smart concrete structures using a resistor mesh model (in English). *Eng Struct* 2017; 148: 924–935.
10. Naem F, Lee HK, Kim HK, et al. Flexural stress and crack sensing capabilities of MWNT/cement composites (in English). *Compos Struct* 2017; 175: 86–100.
11. Jang SH and Yin HM. Effect of aligned ferromagnetic particles on strain sensitivity of multi-walled carbon nanotube/polydimethylsiloxane sensors (in English). *Appl Phys Lett* 2015; 106(14): 141903-1-4.
12. Shindo Y, Kuronuma Y, Takeda T, et al. Electrical resistance change and crack behavior in carbon nanotube/polymer composites under tensile loading (in English). *Compos B Eng* 2012; 43(1): 39–43.
13. Lee E and Jeong YG. Preparation and characterization of sulfonated poly(1,3,4-oxadiazole)/multi-walled carbon nanotube composite films with high performance in electric heating and thermal stability (in English). *Compos B Eng* 2015; 77: 162–168.
14. Sibinski M, Jakubowska M and Sloma M. Flexible temperature sensors on fibers (in English). *Sensors* 2010; 10(9): 7934–7946.
15. Neitzert HC, Vertuccio L and Sorrentino A. Epoxy/MWCNT composite as temperature sensor and electrical heating element (in English). *IEEE Trans Nanotechnol* 2011; 10(4): 688–693.
16. Karimov KS, Mahroof-Tahir M, Saleem M, et al. Temperature sensor based on composite film of vanadium complex (VO<sub>2</sub>(3-fl)) and CNT (in English). *J Semi* 2015; 36(7): 073004-1-5.
17. Chu H, Zhang Z, Liu Y, et al. Self-heating fiber reinforced polymer composite using meso/macropore carbon nanotube paper and its application in deicing (in English). *Carbon* 2014; 66: 154–163.
18. Jeong YG and Jeon GW. Microstructure and performance of multiwalled carbon nanotube/m-aramid composite films as electric heating elements (in English). *ACS Appl Mater Int* 2013; 5(14): 6527–6534.
19. Blasdel NJ, Wujcik EK, Carletta JE, et al. Fabric nanocomposite resistance temperature detector (in English). *IEEE Sens J* 2015; 15(1): 300–306.
20. Galao O, Banon L, Baeza FJ, et al. Highly conductive carbon fiber reinforced concrete for icing prevention and curing (in English). *Materials* 2016; 9(4): 281-1-14.
21. Chang L, Friedrich K, Ye L, et al. Evaluation and visualization of the percolating networks in multi-wall carbon nanotube/epoxy composites (in English). *J Mater Sci* 2009; 44(15): 4003–4012.
22. Feng C and Jiang L. Micromechanics modeling of the electrical conductivity of carbon nanotube (CNT)-polymer nanocomposites (in English). *Compos A Appl Sci Manuf* 2013; 47: 143–149.
23. Garcia-Macias E, D'Alessandro A, Castro-Triguero R, et al. Micromechanics modeling of the electrical conductivity of carbon nanotube cement-matrix composites (in English). *Compos B Eng* 2017; 108: 451–469.
24. Bekyarova E, Itkis ME, Cabrera N, et al. Electronic properties of single-walled carbon nanotube networks (in English). *J Am Chem Soc* 2005; 127(16): 5990–5995.
25. Zhang D, Ryu K, Liu X, et al. Transparent, conductive, and flexible carbon nanotube films and their application in organic light-emitting diodes (in English). *Nano Lett* 2006; 6(9): 1880–1886.
26. Mohiuddin M and Van Hoa S. Electrical resistance of CNT-PEEK composites under compression at different temperatures (in English). *Nano Res Lett* 2011; 6(1): 419-1-5.
27. Xiang ZD, Chen T, Li ZM, et al. Negative temperature coefficient of resistivity in lightweight conductive carbon nanotube/polymer composites (in English). *Macromol Mater Eng* 2009; 294(2): 91–95.
28. Chu K, Lee SC, Lee S, et al. Smart conducting polymer composites having zero temperature coefficient of resistance (in English). *Nanoscale* 2015; 7(2): 471–478.
29. Park I, Li ZY, Pisano AP, et al. Selective surface functionalization of silicon nanowires via nanoscale Joule heating (in English). *Nano Lett* 2007; 7(10): 3106–3111.
30. Kwok N and Hahn HT. Resistance heating for self-healing composites (in English). *J Compos Mater* 2007; 41(13): 1635–1654.
31. Chien AT, Cho S, Joshi Y, et al. Electrical conductivity and Joule heating of polyacrylonitrile/carbon nanotube composite fibers (in English). *Polymer* 2014; 55(26): 6896–6905.
32. Wu JM, Liu JG and Yang F. Three-phase composite conductive concrete for pavement deicing (in English). *Construct Build Mater* 2015; 75: 129–135.
33. Gomis J, Galao O, Gomis V, et al. Self-heating and deicing conductive cement. Experimental study and modeling (in English). *Construct Build Mater* 2015; 75: 442–449.